



# Synthesis and characterization of hyperbranched polyethylenes containing cross-linking structures by chain walking copolymerization of ethylene with diacrylate comonomer

Jianding Ye<sup>a</sup>, Zhibin Ye<sup>a,\*</sup>, Shiping Zhu<sup>b</sup>

<sup>a</sup> School of Engineering, Laurentian University, 935 Ramsey Lake Road, Sudbury, Ontario P3E 2C6, Canada

<sup>b</sup> Department of Chemical Engineering, McMaster University, Hamilton, Ontario L8S 4L7, Canada

## ARTICLE INFO

### Article history:

Received 24 March 2008

Received in revised form 25 May 2008

Accepted 7 June 2008

Available online 13 June 2008

### Keywords:

Hyperbranched polyethylene

Cross-linking

Chain walking polymerization

## ABSTRACT

We report the synthesis of higher-molecular-weight hyperbranched polyethylenes containing cross-linking structures via chain walking copolymerization of ethylene with a diacrylate cross-linker, 1,4-butanediol diacrylate, using a Pd-diimine catalyst,  $[(ArN=C(Me)-(Me)C=NAr)Pd(CH_3)(NCMe)]SbF_6$  ( $Ar = 2,6-(iPr)_2C_6H_3$ ). The hyperbranched chain topology of these polymers was achieved through the chain walking mechanism of the Pd-diimine catalyst. By controlling the diacrylate feed concentration in the polymerization system, three sets of hyperbranched polyethylenes having various cross-linking levels (including both intermolecular and intramolecular cross-linking) but without macrogelation were synthesized at three different temperatures, 15, 25, and 35 °C, respectively. The diacrylate content and cross-linking density in the copolymers were found to increase with the enhancements of diacrylate feed concentration and polymerization temperature. Triple-detection gel permeation chromatography (GPC) measurements confirmed the significant enhancement of polymer average molecular weight and broadening in molecular weight distribution with an increase of diacrylate feed concentration as a result of intermolecular cross-linking. The chain topology of the copolymers becomes more compact, compared to homopolymers, due to the presence of intermolecular cross-linking. Rheological studies show that the copolymers possess characteristic rheological properties typically found in polymers containing intermolecular cross-linking. Our results also indicate qualitatively the presence of intramolecular cross-linking in these hyperbranched copolymers, particularly in those synthesized at 35 °C, probably due to their highly compact chain topologies. This work demonstrates the capability of chain walking polymerization for synthesis of hyperbranched polyethylenes of enhanced molecular weights with the simple use of diacrylate as a cross-linker.

© 2008 Elsevier Ltd. All rights reserved.

## 1. Introduction

Over the past two decades, hyperbranched polymers have received extensive research attention as a new class of polymers of unique chain structure. Distinct from their linear analogues, hyperbranched polymers have structures and topologies similar to those of dendrimers, and possess some strikingly superior material properties, such as low solution/melt viscosity, enhanced solubility, abundance in terminal group, etc. [1]. But, unlike dendrimers that often require tedious synthetic procedures [2], hyperbranched polymers are more easily produced in a large scale [1], which encourages their potential use in a variety of important applications, including rheological additives [3,4], toughening agents [5], drug delivery [6], etc. Traditionally, hyperbranched polymers are

synthesized through condensation polymerization approaches with  $AB_x$ -type multi-functional monomers and, more recently, through a “self-condensing” approach with the use of various inimers [7]. In these synthetic approaches, the hyperbranched chain structure is created through the use of the specially designed functional monomers.

Chain walking ethylene polymerization with Pd-diimine catalysts represents a newly evolved strategy for synthesis of hyperbranched polyethylenes [8]. In this strategy, the control of polymer chain topology is achieved uniquely through the intrinsic chain walking mechanism of the late transition metal catalysts with the simple and commercially abundant ethylene as monomer. This is in sharp contrast to the conventional synthetic approaches that often require specially synthesized functional monomers. Moreover, this strategy allows a convenient tuning of polymer chain topology from linear to moderately branched to hyperbranched by a simple adjustment of polymerization conditions, such as ethylene pressure

\* Corresponding author. Tel.: +1 705 675 1151x2343; fax: +1 705 675 4862.  
E-mail address: [zye@laurentian.ca](mailto:zye@laurentian.ca) (Z. Ye).

and reaction temperature [8–10]. Due to their reduced oxophilicity, Pd-diimine catalysts also possess high tolerance towards polar functional groups, like ester and halide groups, and thus allow the copolymerization of ethylene with polar monomers, typically acrylates and 1-alkenes bearing functional groups, to prepare hyperbranched polyethylenes tethered with various functionalities [11,12].

The molecular weight of hyperbranched polymers is an important parameter directly affecting the polymer properties and end-applications. Developing versatile polymerization strategies, which allow flexible molecular weight control, is important for synthesis of hyperbranched polymers of various molecular weights, particularly high molecular weights, for targeted applications. We have recently explored the potential application of hyperbranched polyethylenes as viscosity index improver in lubricant formulations for the purpose of improving lubricant viscosity index number, an important parameter indicative of lubricant viscosity constancy with temperature [4]. Compared to their linear polymer analogues of similar molecular weights, high-molecular-weight hyperbranched polyethylenes (weight-average molecular weight of about 100 kg/mol) have been found to exhibit tremendously enhanced shear stability, thus enabling the formulated lubricants for high-shear applications. This improvement in shear stability is attributed to their unique highly compact chain topology, which minimizes the shear-induced chain scissions. On the other hand, hyperbranched polyethylenes exhibit compromised viscosity thickening power, the capability in improving lubricant viscosity index, compared to their linear analogues, also as a result of their highly compact topology [4]. Higher polymer concentrations are thus required for these hyperbranched polymers in formulating lubricants of the same viscosity index number. The viscosity thickening power of polymers is sensitively dependent on their molecular weight with higher-molecular-weight polymers giving significantly better thickening power [13]. In order to improve the viscosity thickening power of hyperbranched polyethylenes while maintaining their excellent shear stability, one potential solution is to further increase the molecular weight of polymers while maintaining their highly compact hyperbranched chain topology.

With the condensation polymerization approaches, several efficient strategies have been developed for synthesizing hyperbranched polymers of enhanced molecular weight [14]. In chain walking ethylene polymerization with Pd-diimine catalysts, the effects of polymerization conditions and catalyst structure on molecular weight of the resulting hyperbranched polymer are usually insignificant [9,10]. There is thus limited room to enhance polymer molecular weight by tuning polymerization conditions and/or modifying the catalyst ligand structure. Incorporating cross-linking structures into polymer chains by using a small amount of di- or multi-functional cross-linker during polymerization has often been used to design polymers of novel compact chain topologies (such as cross-linked gels [15], branching structure [16,17], star-shaped topology [18]) and simultaneously enhanced molecular weight. Chain walking ethylene polymerization in the presence of cross-linker is thus a feasible method for obtaining hyperbranched polyethylenes of enhanced molecular weight while with maintained hyperbranched chain structure. In this paper, we report the first study on chain walking ethylene copolymerization with a difunctional diacrylate comonomer, 1,4-butanediol diacrylate, for synthesis of a range of hyperbranched polyethylenes containing various but small quantities of cross-linking structures and having enhanced molecular weight. The effects of cross-linking on polymer molecular weight, chain topology, and rheological properties of the resulting hyperbranched polymers are examined. This work demonstrates the synthesis of hyperbranched polyethylenes of much enhanced molecular weight with the addition of a very small amount of diacrylate as a cross-linker in chain walking ethylene polymerization.

## 2. Experimental section

### 2.1. Materials

All manipulations of air and/or moisture-sensitive compounds were carried out in an N<sub>2</sub>-filled drybox or using Schlenk techniques. The acetonitrile Pd-diimine catalyst, [(ArN=C(Me)–(Me)C=NAr)Pd(CH<sub>3</sub>)(N≡CMe)]SbF<sub>6</sub> (Ar = 2,6-(iPr)<sub>2</sub>C<sub>6</sub>H<sub>3</sub>), was synthesized according to the procedure reported in the literature [19]. Ultra-high purity N<sub>2</sub> and polymer-grade ethylene (both obtained from Praxair) were purified by passing through 3 Å/5 Å molecular sieve and Oxiclear columns to remove moisture and oxygen, respectively, before use. The diacrylate cross-linker, 1,4-butanediol diacrylate (90%, Aldrich), was dried over 4 Å molecular sieves before use. Other chemicals, including anhydrous dichloromethane (99.8%), petroleum ether (ACS reagent grade), triethyl silane (97%), toluene (>99%), methanol (>99%), tetrahydrofuran (THF) (>99%), neutral alumina (~150 mesh), and silica gel (grade 12, 28–200 mesh), were obtained from Aldrich and were used as received.

### 2.2. Chain walking ethylene polymerization

All chain walking ethylene homopolymerizations and copolymerizations with 1,4-butanediol diacrylate were carried out under 1 atm ethylene absolute pressure in a 500 mL jacketed glass reactor equipped with a magnetic stirrer and a temperature-controlled circulating water bath. In a typical run, the glass reactor was first dried overnight at ca. 150 °C in an oven, followed by cooling to room temperature under vacuum, and finally sealed using a rubber septum. The reactor underwent a vacuum–ethylene purge procedure for at least three cycles, and was then pressurized with ethylene at 1 atm (absolute pressure). Subsequently, anhydrous CH<sub>2</sub>Cl<sub>2</sub> (90 mL) and a prescribed amount of 1,4-butanediol diacrylate were injected into the reactor. The reactor temperature was then maintained by passing water through the jacket using the circulating bath set at the designated polymerization temperature. After thermal equilibration for 10 min, the Pd-diimine catalyst (0.1 mmol) dissolved in anhydrous dichloromethane (10 mL) was injected into the reactor to start the polymerization. Ethylene pressure was maintained at 1 atm (absolute) during the polymerization by continuously feeding from a supply line. After a prescribed polymerization time, the polymerization was terminated by venting the reactor and adding triethyl silane (ca. 0.5 mL) under stirring. The polymer was obtained by precipitation in a large amount of methanol followed by further wash with methanol. In order to remove the catalyst residue remaining in the polymer, the dark-colored oily polymer precipitate was redissolved in THF or toluene, and the solution was passed through a column packed with neutral alumina and silica gel. The purified polymer was finally obtained by precipitation in methanol. It was dried overnight under vacuum at room temperature and then weighed.

### 2.3. General procedure for polymer hydrolysis

A general procedure is as follows. A 0.30 g of polymer sample was dissolved in THF (20 mL) in a 250 mL round-bottomed flask equipped with a condenser. To this solution was added NaOH (ca. 1 g) and ethanol (ca. 5 mL), and the mixture was refluxed for ca. 48 h. The solution was then evaporated to dryness and redissolved in THF. The solution was filtrated, and precipitated in methanol. The polymer precipitate was further washed with methanol, and then dried under vacuum to give the hydrolyzed polymer product.

### 2.4. Polymer characterization and analysis

Proton nuclear magnetic resonance (<sup>1</sup>H NMR) analysis of the polymers synthesized was performed on a Varian Gemini 2000

200 MHz spectrometer at ambient temperature. Deuterated chloroform ( $\text{CDCl}_3$ ) was used as the solvent for all the samples for NMR measurement. A high number of scan (generally over 10,000), along with a high polymer sample concentration (about 0.2 g/mL), was used for each polymer analyzed. Differential scanning calorimetry (DSC) analysis of the polymers was performed on a TA Instruments Q100 DSC equipped with a refrigerated cooling system (RCS) under a  $\text{N}_2$  atmosphere. The instrument was operated in the standard DSC mode and was calibrated with an indium standard. A  $\text{N}_2$  purging flow of 50 mL/min was used. Samples (about 5 mg) were heated from room temperature to 150 °C at 20 °C/min and cooled to –85 °C at 10 °C/min, and the data were then collected in the second heating ramp from –85 °C to 150 °C at 10 °C/min. Glass transition temperatures ( $T_g$ ) were read as the middle of the change in heat capacity.

Triple-detection gel permeation chromatography (GPC) measurements were carried out on a Polymer Laboratory PL-GPC220 system equipped with a differential refractive index (DRI) detector (from Polymer Laboratory), a three-angle laser light scattering (LS) detector (high-temperature miniDAWN from Wyatt Technology), and a four-bridge capillary viscosity detector (from Polymer Laboratory). The detecting angles of the light scattering detector were 45, 90, and 135°, and the laser wavelength was 687 nm. One guard column (PL# 1110–1120) and three 30 cm columns (PLgel 10  $\mu\text{m}$  MIXED-B 300  $\times$  7.5 mm) were used. The mobile phase was HPLC-grade THF stabilized with 0.025% BHT and the flow rate was 1.0 mL/min. The GPC system including the column and detector arrays was operated at 30.5 °C. The mass of the polymers injected into the columns varied with polymer molecular weight; typically 200  $\mu\text{L}$  of a 1–4 mg/mL solution was injected. Astra software from Wyatt Technology was used to collect and process the data from all three detectors. Two narrow polystyrene standards from Pressure Chemicals with weight-average molecular weight ( $M_w$ ) of 30,000 and 200,000 g/mol, respectively, were used for the normalization of light scattering signals, and determination of inter-detector delay volume and band broadening. The DRI increment  $dn/dc$  value of 0.078 mL/g, reported in the literature [20], was used for the hyperbranched polyethylenes, and the value of 0.185 mL/g was used for polystyrene.

Rheological characterization of the polymers was carried out on a TA Instrument AR-G2 rheometer. A peltier plate measurement configuration with a 20 mm parallel plate geometry at a gap size of about 1.0 mm was used for the measurements. The measurements were all conducted in the small-amplitude dynamic oscillation mode within the frequency range of 0.001–100 Hz. A strain sweep was performed at 10 Hz before frequency sweeps to establish the linear viscoelastic region for each polymer. The measurements were performed at regular temperature intervals of 10 °C within a temperature range from 15 to 65 °C. Measurement temperature was maintained within  $\pm 0.1$  °C by using the peltier plate temperature control system.

### 3. Results and discussion

#### 3.1. Chain walking copolymerization of ethylene with 1,4-butanediol diacrylate and polymer chain structural elucidation

Due to the capability of Pd-diimine catalysts to incorporate acrylate comonomers [12,21], a commercially available difunctional acrylate monomer, 1,4-butanediol diacrylate, was employed here as the cross-linker in ethylene polymerization. An acetonitrile Pd-diimine complex,  $[(\text{ArN}=\text{C}(\text{Me})-(\text{Me})\text{C}=\text{NAr})\text{Pd}(\text{CH}_3)(\text{N}\equiv\text{C}-\text{Me})]\text{SbF}_6$  ( $\text{Ar} = 2,6\text{-}(\text{iPr})_2\text{C}_6\text{H}_3$ ), was used as the catalyst for polymerization. Attempting to synthesize polymers of hyperbranched chain topology, we used a low ethylene pressure of 1 atm for all polymerization runs following the chain walking mechanism of the Pd-diimine catalysts [8–10]. Table 1 lists the polymerization runs carried out and their corresponding conditions. Three sets of polymers were synthesized by ethylene copolymerization at three different temperatures, 15, 25, and 35 °C, respectively, to investigate the effects of temperature on polymerization behavior and polymer structure. In each set, the feed concentration of diacrylate in the polymerization system was kept low and was increased incrementally from 4.8 mM (corresponding to 0.1 mL diacrylate feed amount in 100 mL polymerization mixture) to a respective maximum concentration (gelation concentration), at which undesired macrogelation occurred during the course of

**Table 1**  
Copolymerization of ethylene with 1,4-butanediol diacrylate and copolymer structural properties

| Run | Sample | $T^{\text{a}}$ (°C) | Diacrylate conc. (mM) | Polymer product (g) | Incorporated diacrylate           |                                     | Cross-linking density <sup>b</sup> (per 1000C) | GPC–LS–VIS charact. |                  |                     |          | Branches <sup>c</sup> (per 1000C) |
|-----|--------|---------------------|-----------------------|---------------------|-----------------------------------|-------------------------------------|--|---------------------|------------------|---------------------|----------|-----------------------------------|
|     |        |                     |                       |                     | Molar content <sup>b</sup> (mol%) | Percent of dual-insert <sup>b</sup> |  | $M_w^c$ (kg/mol)    | PDI <sup>c</sup> | $[\eta]_w^d$ (mL/g) | $\alpha$ |                                   |
| 1   | hPE1   | 15                  | 0                     | 12.5                | 0                                 | 0                                   | 0  | 141                 | 1.50             | 27                  | 0.61     | 103                               |
| 2   | cPE1   | 15                  | 4.8                   | 10.7                | 0.010                             | 36                                  | 0.018  | 253                 | 1.91             | 31                  | 0.49     | 98                                |
| 3   | cPE2   | 15                  | 12                    | 11.4                | 0.027                             | 80                                  | 0.108  | 1,140               | 4.51             | 49                  | 0.39     | 96                                |
| 4   | cPE3   | 15                  | 17                    | Gelled              | –                                 | –                                   | –  | –                   | –                | –                   | –        | –                                 |
| 5   | hPE2   | 25                  | 0                     | 9.7                 | 0                                 | 0                                   | 0  | 142                 | 1.42             | 23                  | 0.58     | 100                               |
| 6   | cPE4   | 25                  | 4.8                   | 8.6                 | 0.011                             | 48                                  | 0.026  | 304                 | 2.05             | 30                  | 0.48     | 100                               |
| 7   | cPE5   | 25                  | 7.2                   | 8.4                 | 0.019                             | 35                                  | 0.033  | 312                 | 2.28             | 28                  | 0.46     | 99                                |
| 8   | cPE6   | 25                  | 12                    | 6.4                 | 0.045                             | 51                                  | 0.11   | 3,029               | 3.89             | 52                  | 0.46     | 95                                |
| 9   | cPE7   | 25                  | 24                    | Gelled              | –                                 | –                                   | –  | –                   | –                | –                   | –        | –                                 |
| 10  | hPE3   | 35                  | 0                     | 8.0                 | 0                                 | 0                                   | 0  | 104                 | 1.48             | 15                  | 0.50     | 101                               |
| 11  | cPE8   | 35                  | 4.8                   | 5.0                 | 0.043                             | 46                                  | 0.10   | 144                 | 1.59             | 16                  | 0.47     | 97                                |
| 12  | cPE9   | 35                  | 12                    | 3.5                 | 0.091                             | 47                                  | 0.21   | 232                 | 1.78             | 18                  | 0.43     | 98                                |
| 13  | cPE10  | 35                  | 24                    | 7.6                 | 0.20                              | 37                                  | 0.37   | 407                 | 2.60             | 21                  | 0.39     | 96                                |
| 14  | cPE11  | 35                  | 36                    | 9.8                 | 0.24                              | 49                                  | 0.59   | 846                 | 4.30             | 28                  | 0.38     | 95                                |
| 15  | cPE12  | 35                  | 48                    | Gelled              | –                                 | –                                   | –  | –                   | –                | –                   | –        | –                                 |
| 16  | cPE13  | 35 (5 h)            | 36                    | 3.5                 | 0.48                              | 34                                  | 0.82   | 144                 | 1.53             | 15                  | 0.40     | 94                                |
| 17  | cPE14  | 35 (10 h)           | 36                    | 6.9                 | 0.29                              | 43                                  | 0.62   | 432                 | 3.40             | 20                  | 0.38     | 95                                |

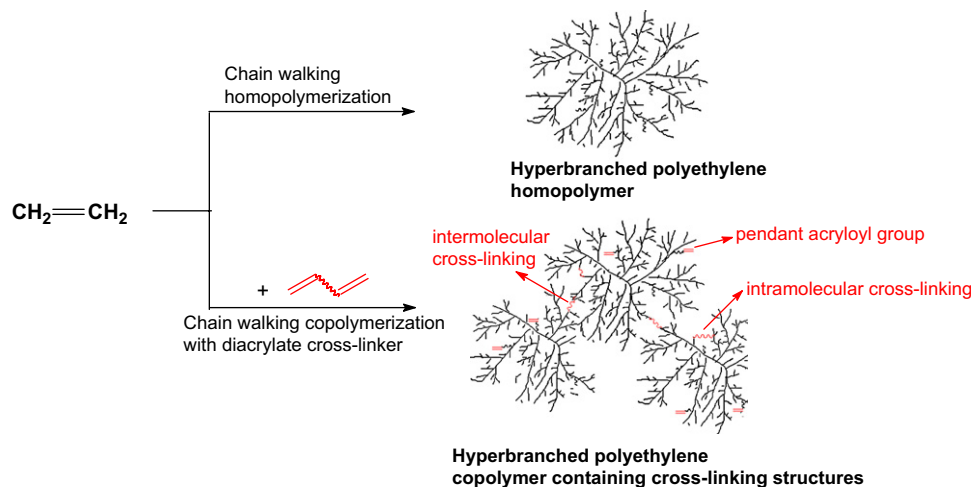
<sup>a</sup> Other polymerization conditions: catalyst, 0.1 mmol; solvent,  $\text{CH}_2\text{Cl}_2$ ; total volume, 100 mL; ethylene pressure, 1 atm; polymerization time, 22 h for Runs 1–15, 5 h for Run 16, and 10 h for Run 17.

<sup>b</sup> The diacrylate molar content, percentage of dual-insertion, and cross-linking density (defined as the number of dual-inserted diacrylate units per 1000 carbons) were determined by using  $^1\text{H}$  NMR spectroscopy (over 10,000 scans at 200 MHz).

<sup>c</sup> The weight-average molecular weight ( $M_w$ ) and polydispersity index (PDI) determined from the light scattering measurements.

<sup>d</sup> Weight-average intrinsic viscosity ( $[\eta]_w$ ) was determined from the viscosity detector.

<sup>e</sup> Branching density of the ethylene sequence determined from  $^1\text{H}$  NMR spectroscopy.



**Scheme 1.** Chain walking ethylene homopolymerization and copolymerization with diacrylate.

polymerization. Macrogelation was found to occur in Runs 4, 9, and 15 with a diacrylate gelation concentration of 17, 24, and 48 mM, respectively. During the course of these three runs, gelation occurred at a certain point when the reaction fluid lost its mobility and the polymerization was terminated. Homopolymerization of ethylene was also carried out in each set as a control run (Runs 1, 5, and 10). For most polymerization runs without the occurrence of macrogelation, a polymerization time of 22 h was adopted. In Runs 16 and 17, a shorter polymerization time of 5 h and 10 h, respectively, was used, while with the other conditions same as Run 14, to investigate the effect of polymerization time on the polymer molecular weight development. Scheme 1 shows schematically the polymerization processes and polymer structures.

The successful incorporation of diacrylate in the polymers is confirmed by polymer structural elucidation using  $^1\text{H}$  NMR spectroscopy. Representatively, Fig. 1 shows the  $^1\text{H}$  NMR spectrum of the copolymer (cPE10 in Table 1) synthesized in Run 13 at 35 °C and with a diacrylate concentration of 24 mM. Besides the three major resonances assigned to methyl, methylene, and methine protons of the ethylene sequences, weak resonance signals (*a*, *b*, *c*, *d*, and *e* labeled in Fig. 1) attributed to the incorporated diacrylate units are observed in the copolymer  $^1\text{H}$  NMR spectrum. These resonances lead to the identification of two expected types of incorporated

diacrylate microstructures (shown in Fig. 1), resulting from the mono-insertion and dual-insertion, respectively, of the diacrylate comonomer. During polymerization, the mono-insertion of a single double bond of the symmetric difunctional comonomer leads to copolymers tethered with pendant acryloyl groups. These copolymers may subsequently serve as macromonomers in successive polymerization, leading to intermolecular cross-linking structure by enchainment of one or more of the pendant acryloyl groups (dual-insertion) into another kinetic polymer chain. Dual-insertion can also occur by intramolecular cross-linking or cyclization with one or more of the pendant acryloyl groups enchainment back into the same primary chain. Therefore, the microstructure resulted from dual-insertion of the diacrylate monomer includes the contributions of both intermolecular and intramolecular cross-linking. However, the two cannot be differentiated from  $^1\text{H}$  NMR spectroscopy, and the percentage of intermolecular cross-linking in these dual-inserted structures, therefore, cannot be determined.

The presence of the pendant acryloyl groups,  $\text{CH}_2=\text{CH}-\text{C}(\text{O})\text{O}-\text{CH}_2-$ , is confirmed from the resonances of the vinyl protons (*d*, *e*) and the methylene protons (*c* at 4.19 ppm) next to the acryloyl functionality. The enchainment of either acryloyl group in the symmetrical diacrylate comonomer leads to a downshift of the most nearby methylene protons from *c* at 4.19 ppm to *b* at 4.10 ppm in the  $^1\text{H}$  NMR spectrum [12], along with the appearance of a new triplet signal (*a*) at 2.30 ppm assigned to the methylene protons of the  $-\text{CH}_2-\text{C}(\text{O})\text{O}-$  group. Integration of resonance *b* is greater than that of resonance *c*, indicating the presence of dual-inserted diacrylate units. The triplet resonance at 2.30 ppm (*a*) suggests that the acrylate functionalities are incorporated at the end of branches (shown in Fig. 1), which is a typical incorporation microstructure for acrylate comonomers in olefin copolymerization with Pd-diimine catalysts [12,21]. The presence of this triplet methylene resonance, which is the only resonance in the region of 2.2–2.5 ppm, also indicates that both incorporated diacrylate structures result from the coordinative insertion mechanism of the Pd-diimine catalyst. Diacrylate monomers are often used as cross-linkers in radical polymerizations. The enchainment of the acrylate double bond through the radical mechanism should result in a methine group, which typically shows resonances in the region of 2.2–2.5 ppm in the polymer  $^1\text{H}$  NMR spectrum [22]. The sole presence of the triplet methylene resonance in the region thus rules out the possible presence of enchainment acrylate units through radical mechanism [23]. The low polymerization temperatures (15–35 °C) used here are too low to induce radical polymerization in a short period of 22 h.

The above characteristic resonances resulting from the incorporated diacrylate units were observed in the  $^1\text{H}$  NMR spectra of

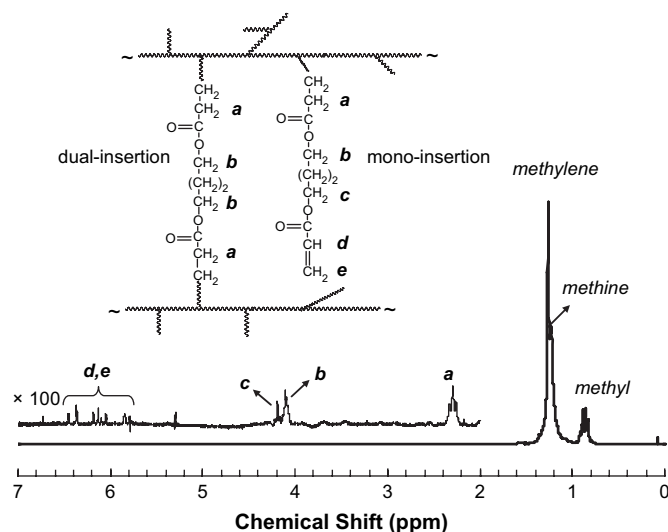


**Fig. 1.**  $^1\text{H}$  NMR spectrum of ethylene-diacrylate copolymer (cPE10 in Table 1) synthesized in Run 13 at 35 °C and with a diacrylate concentration of 24 mM.

all copolymers synthesized, but at different intensities. The diacrylate molar content and the percentage of dual-inserted diacrylate units in each copolymer were calculated from their  $^1\text{H}$  NMR spectra. Cross-linking density, defined here as the number of dual-inserted diacrylate units per 1000 carbons, was also calculated using the molar content and dual-insertion percentage data. Herein, the cross-linking density data include the contributions from both intermolecular and intramolecular cross-linking. These results are all summarized in Table 1. For all copolymers excluding the macro-gelled polymers that were not characterized, the diacrylate molar contents are low, generally less than 0.5%, due to the small amounts of diacrylate employed in the polymerization runs to avoid macrogelation. In each polymer set, the increase of diacrylate feed concentration in the polymerization system gives rise to the enhanced diacrylate molar content and cross-linking density. At the same diacrylate feed concentration, increasing polymerization temperature generally enhances the diacrylate molar content and cross-linking density. However, the dual-insertion percentage data do not show a clear trend of change with either diacrylate concentration or polymerization temperature and are typically in the range of 34–51%. Comparing Run 14 with Runs 16 and 17 having the same polymerization temperature and diacrylate concentration, an increase of the polymerization time from 5 h to 22 h reduces both the diacrylate molar content and the cross-linking density in the copolymers, indicating the shift of copolymer composition with the decreasing diacrylate concentration during the course of polymerization.

The branching densities of the hyperbranched ethylene sequences in the copolymers, generated by chain walking of the catalyst, were calculated using the methyl, methylene, and methine resonances of the ethylene sequences. The results are also listed in Table 1. Regardless of the different polymerization temperatures and diacrylate contents, all the copolymers and homopolymers generally possess very similar branching densities (about 100 branches/1000 carbons). This is commonly observed in hyperbranched copolymers synthesized with Pd-diimine catalysts [12]. It should be noted that the chain topology differences among the polymers cannot be differentiated by  $^1\text{H}$  NMR technique as it only determines the number of methyl groups at the branch ends while the important branch-on-branch structures cannot be detected [8,12]. In each set of polymers synthesized at the same temperature, the amount of polymer produced (listed in Table 1) generally decreases with the increase of diacrylate content. This is due to the formation of a stable Pd-diimine chelate complex following the acrylate enchainment during polymerization, which inhibits next ethylene insertion [21]. Comparing polymers synthesized at the same diacrylate feed concentrations, the amount of polymer produced tends to decrease with the increase of polymerization temperature due to enhanced catalyst decomposition and/or the greater diacrylate incorporation at higher temperatures.

It is interesting to note that the diacrylate gelation concentration, at which macrogelation occurred, increases significantly from 17 mM to 48 mM with the increase of polymerization temperature from 15 to 35 °C. On the basis of Flory–Stockmayer's mean-field theory [24], the critical gel point, at which gelation starts to occur, is reached when the number of intermolecular cross-linking units per primary chain equals unit in the copolymerization of monovinyl monomer and divinyl cross-linker. These three runs with the occurrence of macrogelation should be very close to the critical gel point as gelation did not occur in other runs with slightly lower diacrylate feed concentrations in each set. The significant enhancement of the diacrylate gelation concentration with the temperature increase thus indicate the presence of intramolecular cross-linking in the polymerization and, moreover, its percentage in the dual-inserted cross-linking structures is enhanced significantly with the increase of polymerization temperature from 15 to 35 °C.

Intramolecular cross-linking results from the enchainment of the pendant double bonds into the same primary chain by the catalyst active site. It consumes the pendant double bonds but has no contribution to the increase of polymer molecular weight. It is often neglected in cross-linking modeling studies [15b,24,25]. The occurrence of intramolecular cross-linking often leads to the wastage of cross-linker for efficient intermolecular cross-linking and requires a higher cross-linker concentration than the theoretically predicted value [25]. The occurrence of intramolecular cross-linking requires that the active site of the growing chain and the pendant double bonds on the same chain are in close vicinity. We envisage intramolecular cross-linking is enhanced in hyperbranched polymers herein studied, compared to linear polymers, owing to their much more compact chain topology, which brings catalyst active site and the pendant double bonds on the same growing chain to much closer vicinity. As will be shown in the next section, the chain topology of the hyperbranched polyethylene synthesized in chain walking polymerization becomes increasingly hyperbranched and compact with the increase of polymerization temperature following the chain walking mechanism of Pd-diimine catalysts. The increasingly hyperbranched polymer chain topology generated at higher polymerization temperatures thus further enhances the intramolecular cross-linking, which consequentially gives rise to a higher diacrylate gelation concentration with the temperature increase found here.

Due to their highly branched nature, all the polymers without macrogelation have good solubility in solvents like THF, toluene, etc. even at room temperature. The gelled polymers were not characterized in this study as they are not the target of this work. In each set of polymers, the physical appearance of the polymers changes tremendously from low-viscosity oil-like liquids to sticky elastic solids of very high viscosity with the increase of diacrylate content in the copolymer. DSC measurements were carried out to study the thermal properties of the polymers. Representatively, Fig. 2 shows the DSC thermogram of the copolymer (cPE11) produced in Run 14 at 35 °C and a diacrylate concentration of 36 mM, which has the highest diacrylate content among all the copolymers synthesized, along with that of the corresponding control homopolymer (hPE3) synthesized in Run 10 for comparison. The diacrylate incorporation, however, does not seem to have an apparent effect on polymer thermal transitions due to its low molar content (only 0.24%). Both polymers possess a glass transition at about  $-67.5$  °C and a weak endotherm with peak maximum at about  $-32.9$  °C, which is probably a melting endotherm resulting from the highly branched polyethylene sequences [12].

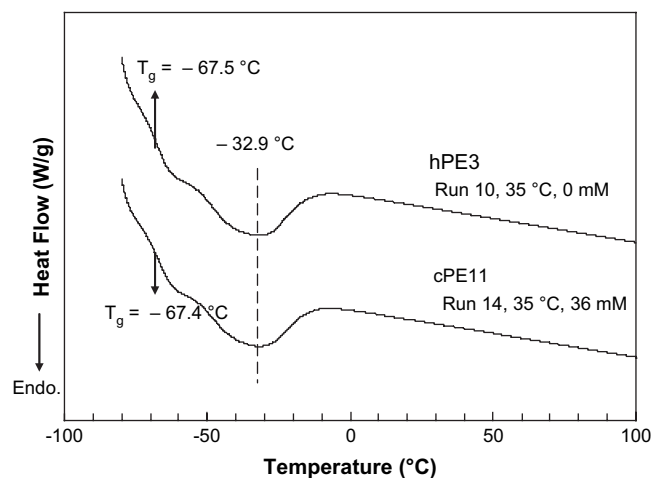
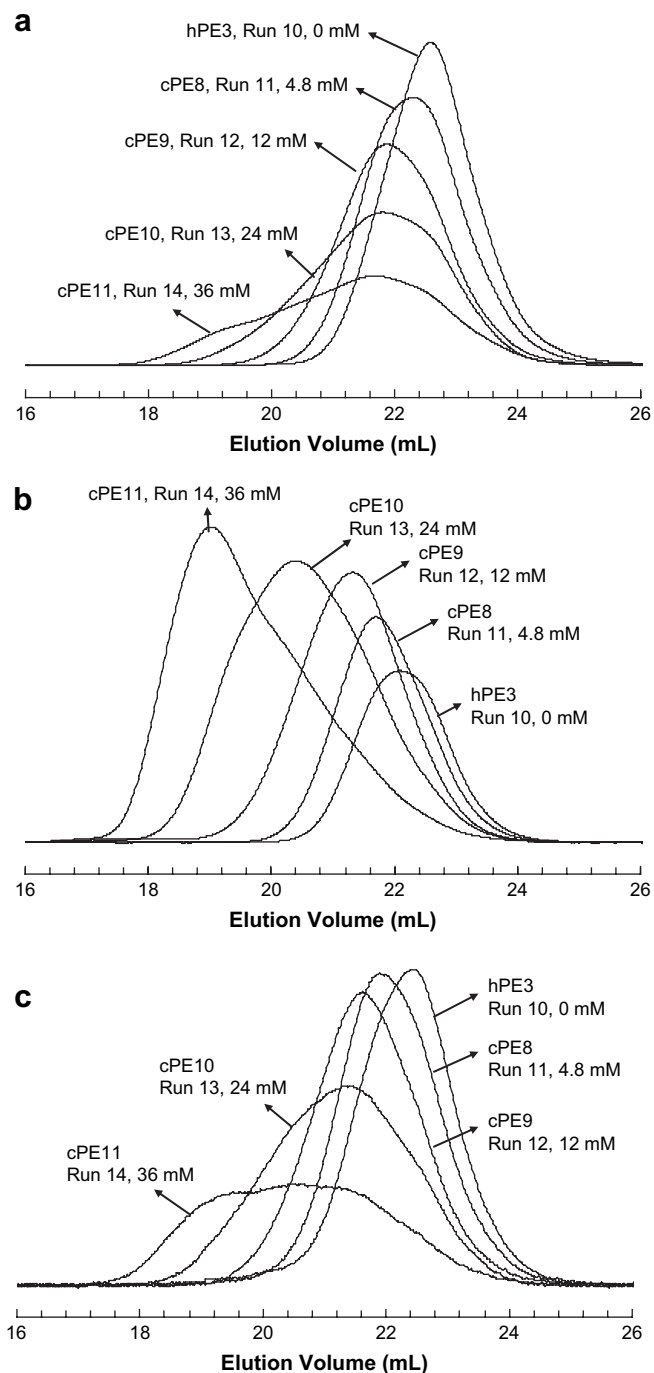


Fig. 2. Differential scanning calorimetry thermograms for the polymers (hPE3 and cPE11) synthesized at 35 °C and with a diacrylate feed concentration of 0 and 36 mM, respectively (Runs 10 and 14 in Table 1).

### 3.2. Polymer characterization with triple-detection GPC

Triple-detection GPC equipped with online differential refractive index (DRI), three-angle light scattering (LS), and capillary viscosity detectors was applied to characterize polymer molecular weight and distribution, dilute solution properties, and chain topology. Representatively, Fig. 3 shows the GPC elution curves obtained from the three respective detectors for the set of polymers synthesized at 35 °C with varying diacrylate concentrations. As shown in Fig. 3a, GPC elution curves recorded from the DRI detector



**Fig. 3.** Gel permeation chromatography elution traces recorded using (a) differential refractive index detector (relative concentration), (b) light scattering detector (Rayleigh ratio at 90° detecting angle), and (c) the viscosity detector (specific viscosity) for the set of polymers synthesized at 35 °C with different diacrylate concentrations (Runs 10–14 in Table 1).

show increasingly pronounced tailing to shorter retention times (higher molecular weights) and broadening with increasing diacrylate feed concentration. The peak maxima also shift to shorter retention times with increasing diacrylate feed concentration. Moreover, for cPE11 synthesized at the highest diacrylate concentration in the set, the curve exhibits bimodal distribution. Fig. 3b shows the GPC elution curves obtained from the LS detector (90° detection angle), which is significantly more sensitive to the presence of higher-molecular-weight chains. In the polymer set, the elution curves shift significantly towards shorter retention times with increasing diacrylate concentration. These results confirm the increasing number of intermolecular cross-linking units in the copolymers with the increase of diacrylate feed concentration. Similar trends of changes of GPC elution traces with the increase of diacrylate feed concentration were also observed with the other two sets of polymers synthesized at 15 and 25 °C, respectively. For the purpose of brevity, their GPC elution traces are not illustrated here, but are included in Supplementary data.

Using the DRI and three-angle LS detectors, the absolute molecular weight data of the polymers were determined. The weight-average molecular weight ( $M_w$ ) and polydispersity index (PDI) data calculated from the light scattering signals are listed in Table 1. The incorporation of a small amount of diacrylate has been found to be very effective in enhancing polymer molecular weight. In each set of polymers synthesized at the same temperature, both  $M_w$  and PDI data increase significantly with the increase of diacrylate feed concentration, indicating the increasing amount of intermolecular cross-linking involved. For instance, the copolymer (cPE6), synthesized in Run 8 at 25 °C with a low diacrylate feed concentration of 12 mM, possesses a high  $M_w$  of 3029 kg/mol and a PDI of 3.89 compared to a  $M_w$  of 142 kg/mol and a PDI of 1.42 for the homopolyethylene control sample (hPE2 from Run 5). Polymerization time was also found to be important for polymer molecular weight development. Fig. 4 compares the GPC elution curves for the set of polymers (cPE11, cPE13, and cPE14) synthesized with varying polymerization time at 35 °C and the same diacrylate feed concentration of 36 mM. With the increase of polymerization time from 5 h to 22 h, the GPC elution curves shift consistently towards the shorter elution time and become broader. As shown in Table 1, the  $M_w$  and PDI data are significantly enhanced with the increase of polymerization time. These results reflect that the double-bond-containing polymers, produced in the earlier stage of polymerization, continue to serve as macromonomers for further intermolecular cross-linking reactions, which increases polymer molecular weight at extended polymerization time.

The presence of intramolecular cross-linking in these hyper-branched copolymers is also evidenced by comparing the molecular weight data for the polymers containing a similar cross-linking density value in the three sets. The three polymers, cPE2, cPE6, and cPE8, have a similar cross-linking density of 0.11 per 1000 carbons (Table 1). Both cPE2 and cPE6 possess significantly enhanced  $M_w$  and broadened PDI compared to their corresponding homopolymer while cPE8 synthesized at 35 °C only show marginal increase in both  $M_w$  and PDI. If they contained a similar level of intermolecular cross-linking, comparable increases in  $M_w$  and PDI should be expected for cPE8. Furthermore, hydrolysis experiments were carried out on the three polymers to cleave the ester linkages. For polymers containing mostly intermolecular cross-linking, the hydrolysis process should result in polymers with significantly reduced molecular weight. For polymers containing mainly intramolecular cross-linking, the process should not affect the polymer molecular weight significantly. Fig. 5 compares, respectively, the GPC elution traces (from DRI detector) of the three polymers before and after hydrolysis. For bimodal-distributed cPE2 and cPE6, the higher-molecular-weight peak disappears and the elution curve turns out to be monomodal after the hydrolysis, indicating the

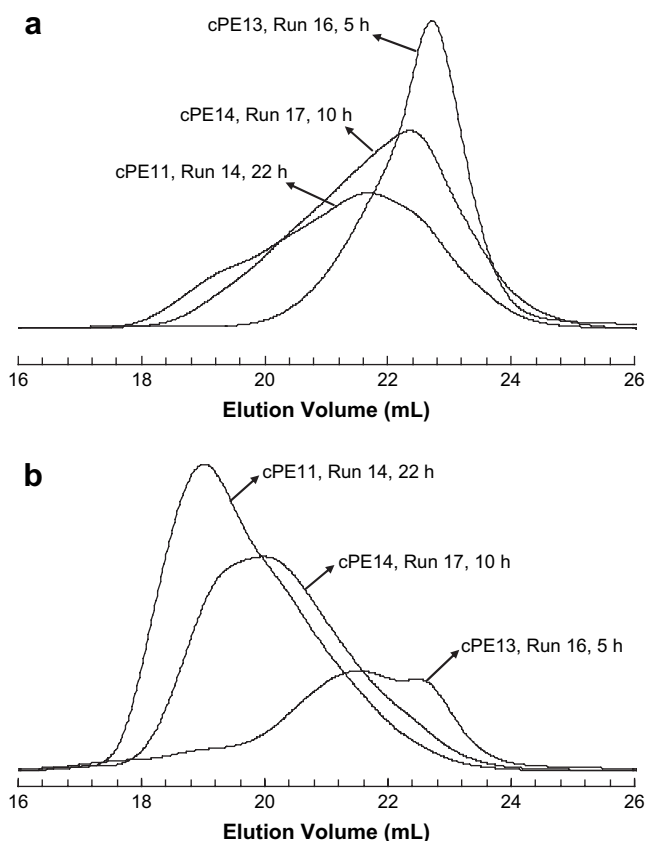


**Fig. 4.** Gel permeation chromatography elution traces recorded using (a) differential refractive index detector (relative concentration) and (b) light scattering detector (Rayleigh ratio at 90° detecting angle) for polymers synthesized with different polymerization time at 35 °C and diacrylate concentration of 36 mM (Runs 14, 16 and 17 in Table 1).

significant presence of intermolecular molecular cross-linking in these two polymers. The elution curve for cPE8, however, does not significantly change after the hydrolysis process. This tremendous difference also confirms the predominant presence of intramolecular cross-linking in cPE8 and indicates the level of intramolecular cross-linking is enhanced with the increase of polymerization temperature at a given diacrylate feed concentration.

When coupled with the DRI detector, the viscosity detector of the triple-detection GPC allows the determination of polymer intrinsic viscosity,  $[\eta]$ , for each GPC eluting fraction. Representatively, the GPC elution curves obtained from the viscosity detector for the set of polymers (Runs 10–14) synthesized at 35 °C are shown in Fig. 3c. Like those recorded from DRI and LS detectors, the elution curves broaden significantly and shift to shorter elution time with the increase of diacrylate feed concentration in polymerization. The weight-average intrinsic viscosity ( $[\eta]_w$ ) data calculated for the polymers are listed in Table 1. Fig. 6 shows the Mark–Houwink plots (intrinsic viscosity vs molecular weight plots) for the three sets of polymers synthesized at the three different temperatures. In these plots, the molecular weight data are the absolute ones determined by the light scattering detector. The Mark–Houwink  $\alpha$  values, corresponding to the slopes of the curves in the double-log plot, are listed in Table 1.

Comparing the three homopolymers (hPE1, hPE2, and hPE3), consistent downshifts of the intrinsic viscosity curves are observed with the increase of polymerization temperature from 15 to 35 °C (Fig. 6a), suggesting that the polymer produced at a higher temperature possesses more compact polymer chain topology [9]. The Mark–Houwink  $\alpha$  value of the homopolymers is reduced from 0.61 to 0.50 with the temperature increase, which is also indicative of

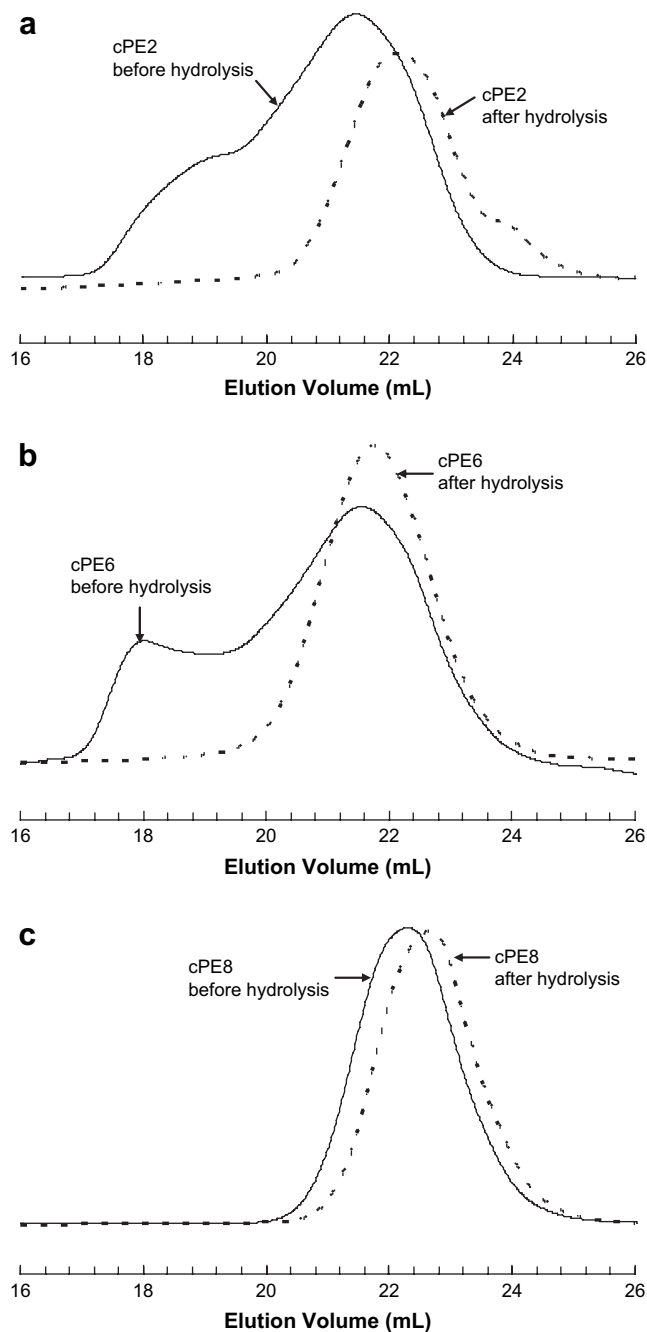


**Fig. 5.** Gel permeation chromatography elution traces (from differential refractive index detector) of the polymers before and after hydrolysis: (a) cPE2, (b) cPE6, and (c) cPE8.

increasingly compact polymer chain conformation generated at higher temperatures [17b]. These results are in consistency with the chain walking mechanism of Pd–diimine catalysis. In the two sets of polymers synthesized at 15 and 25 °C, respectively, the copolymers containing incorporated diacrylate units exhibit reduced  $[\eta]$  values, particularly at the high-molecular-weight end, compared to their corresponding homopolyethylene control sample (Fig. 6a and b). The reduction is more pronounced with the polymer containing a higher diacrylate content and is indicative of the increasingly compact polymer chain conformation. As shown in Table 1, the Mark–Houwink  $\alpha$  value also decreases with the increase of diacrylate content in each set.

Reductions in intrinsic viscosity and  $\alpha$  value have often been observed in polymers containing intermolecular cross-linking

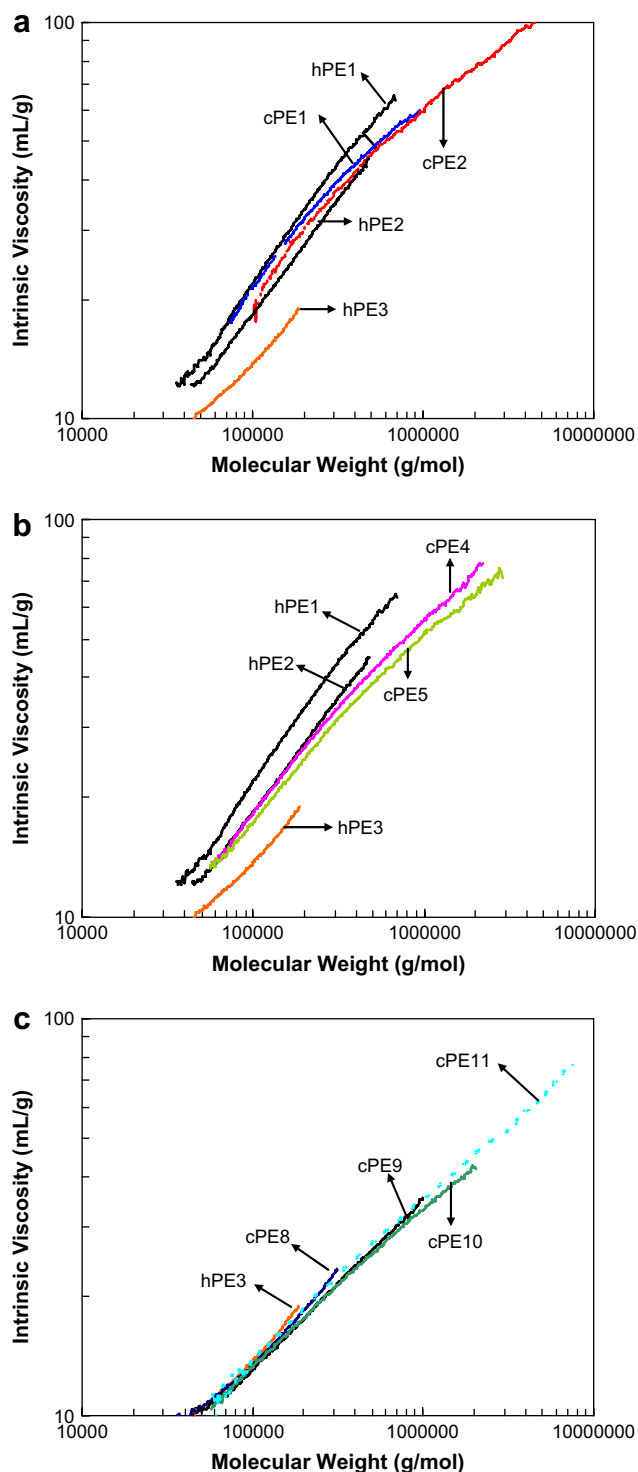


**Fig. 6.** Intrinsic viscosity vs molecular weight plot for (a) the set of polymers synthesized at 15 °C (Runs 1–3), (b) the set of polymers synthesized at 25 °C (Runs 5–7), and (c) the set of polymers synthesized at 35 °C (Runs 10–14). In (a) and (b), the curves for homopolymers synthesized at the other temperature levels are also included for comparison.

structures [17,18]. Intramolecular cross-linking at high levels has also been shown to lead to more compact dendrimers [26]. However, these reductions herein should result primarily from intermolecular cross-linking as the reduction in  $[\eta]$  occurs mainly in the high-molecular-weight region, where intermolecular cross-linking is significant. The effect of intramolecular cross-linking on chain conformation should be weak as the intramolecular cross-

linking level should be low given the low diacrylate contents of the polymers. For the set of polymers synthesized at 35 °C at various diacrylate concentrations, the effect of diacrylate incorporation on the Mark–Houwink curves, however, is not as significant as those observed in the other two sets of polymers in spite of their higher diacrylate contents (Fig. 6c). The significantly more compact chain conformation of this set of polymers, compared to the other two sets, probably renders them with the reduced sensitivity of chain conformation change towards the intermolecular cross-linking. But reductions in  $\alpha$  values are apparent as shown in Table 1. These Mark–Houwink conformation plots thus confirm that the copolymers have maintained (and even slightly enhanced for the sets of polymers synthesized at 15 and 25 °C) highly compact hyperbranched chain structure compared to the homopolyethylene control samples in spite of their enhanced molecular weights due to intermolecular cross-linking.

### 3.3. Polymer rheological characterization

Small-amplitude dynamic oscillatory melt rheological measurements were conducted on this series of hyperbranched polymers to study the effects of cross-linking on their rheological behaviors. The measurements were all carried out in the respective linear viscoelastic region of each polymer melt. Low measurement temperatures, typically in the range from 15 to 65 °C, were used to minimize the possible thermal-initiated further cross-linking in the copolymers containing pendant acryloyl groups during measurements. The incorporation of diacrylate units in the polymers, though at low levels, significantly affects the rheological properties of the hyperbranched polymers due to the formation of intermolecular cross-linking. Some typical rheological behaviors characteristic of polymers containing intermolecular cross-linking structures were found with this series of hyperbranched polymers. The representative rheological properties of the set of polymers synthesized at 35 °C with various diacrylate feed concentrations are herein reported to demonstrate the effects of intermolecular cross-linking. Similar effects were found with the other two sets of polymers. For the purpose of brevity, their rheological properties are included into [Supplementary data](#).

Fig. 7 shows the dynamic modulus curves measured at 25 °C for the set of polymers synthesized at 35 °C. The homopolymer in this set, hPE3, exhibited as an oil-like liquid showing mainly viscous behavior. In the whole frequency range,  $G''(\omega)$  is always dominant over  $G'(\omega)$  with no crossover. The rheological properties of homopolymers synthesized with Pd-diimine catalysts at different

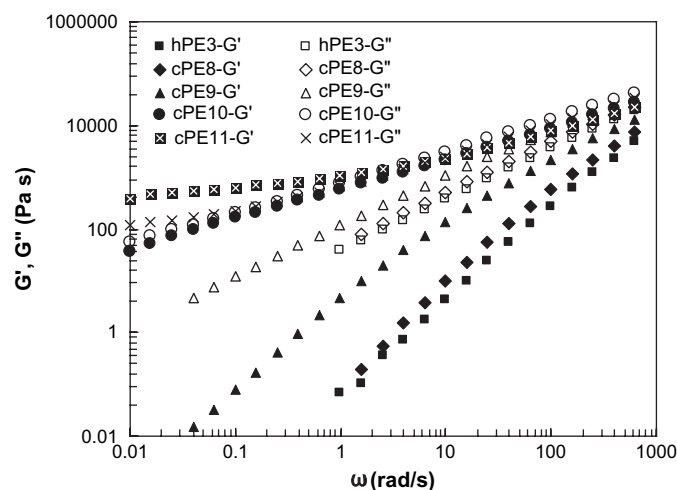


**Fig. 7.**  $G'(\omega)$  and  $G''(\omega)$  curves measured at 25 °C for the set of polymers synthesized at 35 °C.



conditions have been reported in our prior studies [12a]. With the increase of diacrylate content in the copolymer, both  $G'(\omega)$  and  $G''(\omega)$  curves are raised significantly. For the polymers containing a relatively lower cross-linking density (cPE8 and cPE9),  $G''(\omega)$  is still dominant over  $G'(\omega)$  within the whole frequency range with no crossover observed, indicating that the polymers, like the homopolymer control, are still predominantly viscous. For cPE10 having a higher diacrylate content, the two curves are almost parallel in the whole frequency range with the  $G'(\omega)$  curve slightly below the  $G''(\omega)$  curve without crossover. For cPE11 having the highest diacrylate content in this set, a rubbery plateau at low frequencies with  $G'(\omega) > G''(\omega)$  is observed, while it is mainly viscous with  $G'(\omega) < G''(\omega)$  at the high frequencies, and a crossover point between the two curves is found at  $\sim 10$  rad/s. Moreover, the left side of the  $G'(\omega)$  curve tends to reach an equilibrium modulus ( $G_e$ ) with the decrease of frequency, which is typically found with intermolecular cross-linked polymers [27]. Similar trends of change of the dynamic modulus curves with the increase of diacrylate content were also observed with the other two sets of polymers, indicating an increasing level of intermolecular cross-linking in the polymers having a higher diacrylate content.

Fig. 8 compares the  $\log G'$  vs  $\log G''$  master curves for the set of polymers synthesized at 35 °C. These master curves are plotted using the data obtained at various measurement temperatures from 15 to 55 °C. The curves show very weak dependence on measurement temperatures and all the data obtained at various measurement temperatures for each polymer can be described by a single master curve [16]. Comparing the set of polymers, a consistent up-shift of the  $\log G'$  vs  $\log G''$  curve is found relative to the respective homopolyethylene control sample and it becomes more pronounced with polymers having a higher diacrylate content. Such up-shifted  $\log G'$  vs  $\log G''$  curves are often found with polymers containing intermolecular cross-linking structures and long-chain branched polymers, and are indicative of the increasingly enhanced elasticity in these polymers [16,28]. Fig. 9 shows the complex viscosity curves measured at 25 °C for the set of polymers. The incorporation of a very small amount of diacrylate (up to 0.24%) has significantly changed the complex viscosity curves due to the presence of both intermolecular cross-linking structure and the enhanced  $M_w$ . With the increase of diacrylate content, the complex viscosity in the low-frequency range increases tremendously and shear-thinning becomes more pronounced. For polymers of the highest diacrylate content in the set (cPE10 and cPE11), the Newtonian viscosity plateau at the low-frequency end could not be reached in our experimental frequency range while it is still present in copolymers containing a relatively lower diacrylate content (cPE8 and cPE9).

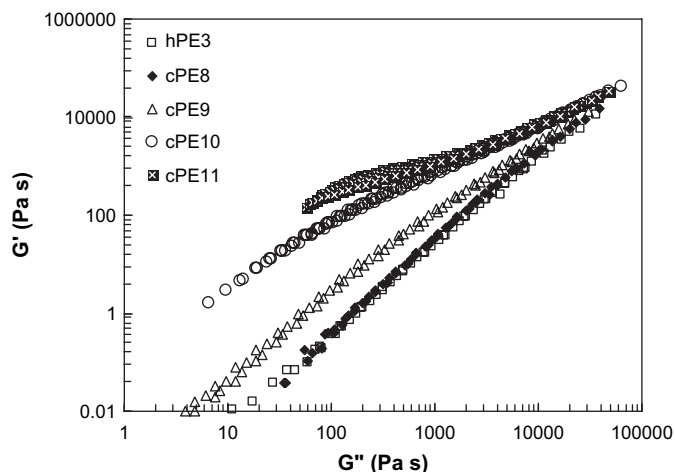


Fig. 8.  $\log G'$  vs  $\log G''$  master curves for the set of polymers synthesized at 35 °C.

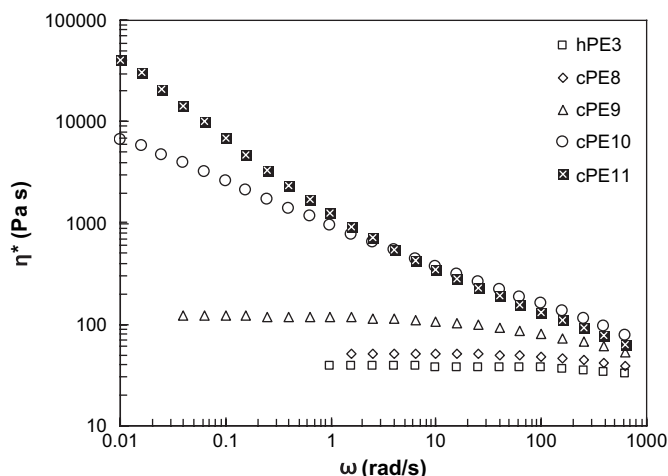


Fig. 9. Complex viscosity curves measured at 25 °C for the set of polymers synthesized at 35 °C.

Fig. 10 shows the phase angle curves for the set of polymers at the measurement temperature of 25 °C. The polymers containing cross-linking structure exhibit reduced phase angles compared to the homopolyethylene control sample within the frequency range investigated. With the increase of diacrylate content, the reduction is more pronounced and a consistent change in the shape of the phase angle curves is found due to the added long-time relaxation mode from the intermolecular cross-linked polymers in the viscoelastic behavior.

The temperature-dependences of the viscoelastic properties of the polymers were investigated. The three hyperbranched homopolyethylene control samples (hPE1–hPE3) were found to obey the time–temperature superposition with a similar Arrhenius activation energy of about 52 kJ/mol. These hyperbranched homopolymers are thus thermorheologically simple. Fig. 11 shows the Van Gurp's plots (phase angle vs  $\log G^*$ ) for the set of polymers synthesized at 35 °C. Van Gurp's plot has often been used to evaluate polymer thermorheological complexity [12a,16,28b]. For a thermorheologically simple polymer, all the data obtained at various temperatures should fall into a single smooth curve in the plot while scattering of the data is often observed with thermorheologically complex polymers that violate the time–temperature superposition [12a,16,28b]. As shown in Fig. 11, the data measured at different temperatures for the homopolymer (hPE3) superpose

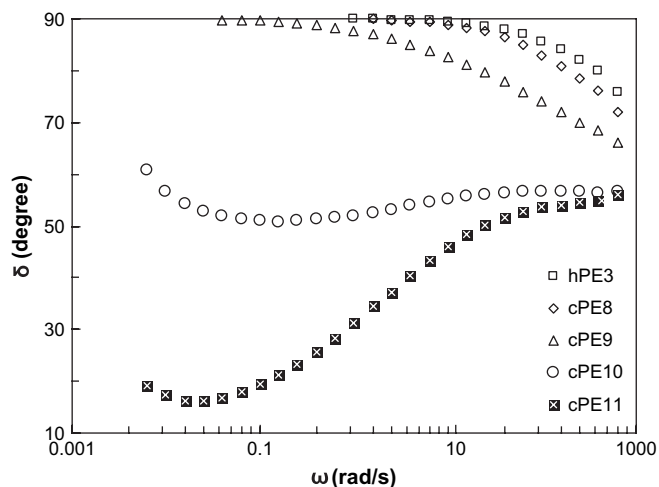


Fig. 10. Phase angle curves measured at 25 °C for the set of polymers synthesized at 35 °C.

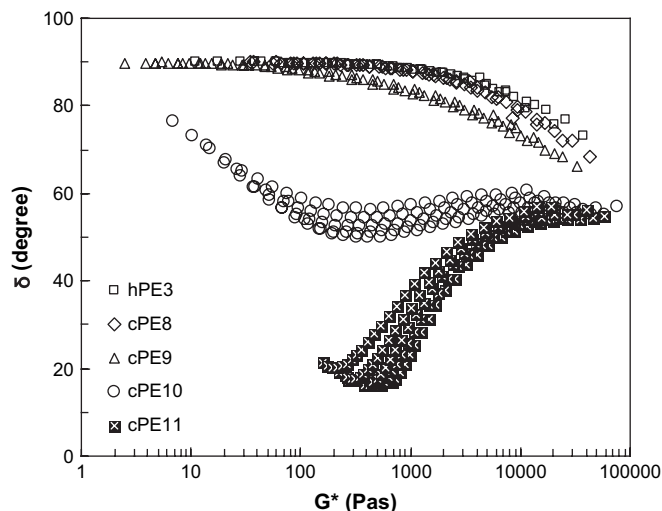


Fig. 11. Van Gurp's plots for the set of polymers synthesized at 35 °C.

very well by falling into a single smooth curve in this plot. For copolymers containing a lower diacrylate content (such as cPE8 and cPE9), smooth lines are also found and the scattering of the data is not apparent, indicating that they still obey the time–temperature superposition. However, for copolymers having a higher diacrylate content (cPE10 and cPE11), the data are significantly scattered, thus violating the time–temperature superposition and being thermorheologically complex. Such thermorheological complexity has often been found with polymers containing intermolecular cross-linking structure and is a result of constraints imposed by intermolecular cross-linking points on chain relaxation [12a,16,28b].

For thermorheologically simple polymers, the temperature dependence of modulus shift factor,  $a_T$ , follows the Arrhenius relation over relatively narrow temperature ranges far from the polymer glass transitional temperature [27]. The flow activation energy,  $E_a$ , which is a measure of temperature sensitivity of rheological properties, is given by

$$a_T = \exp \left[ \frac{E_a}{R} \left( \frac{1}{T} - \frac{1}{T_0} \right) \right] \quad (1)$$

where  $R$  is the universal gas constant and  $T_0$  is the reference temperature. Thermorheologically complex polymers, however, do not follow this simple relation. These polymers do not have single activation energy but exhibit modulus-dependent temperature sensitivity [29]. Fig. 12 shows the activation energy spectra of the set of polymers synthesized at 35 °C. These spectra were calculated from the experimental storage modulus data ( $G'(\omega)$ ), measured at various temperatures, according to the method summarized by Wood-Adams and Costeux [29]. For thermorheologically simple homopolymers and copolymers having relatively lower diacrylate contents in each set (cPE9), the activation energy remains approximately constant over broad frequency ranges. But the incorporation of cross-linking structure seems to slightly raise the activation energy value compared to the homopolymer control sample. The spectra for the thermorheologically complex copolymers having higher diacrylate contents (i.e., higher levels of intermolecular cross-linking structure) are, however, very different. High activation energies (up to 95 kJ/mol for cPE11) are found at low-frequency values. From the trend of the spectra for these polymers, even higher activation energies should be found at further reduced frequency values, which were somehow difficult to achieve in the measurements. With the increase of frequency, the activation energy decreases significantly and reaches an equilibrium value of about 52 kJ/mol at the high-frequency end, which is

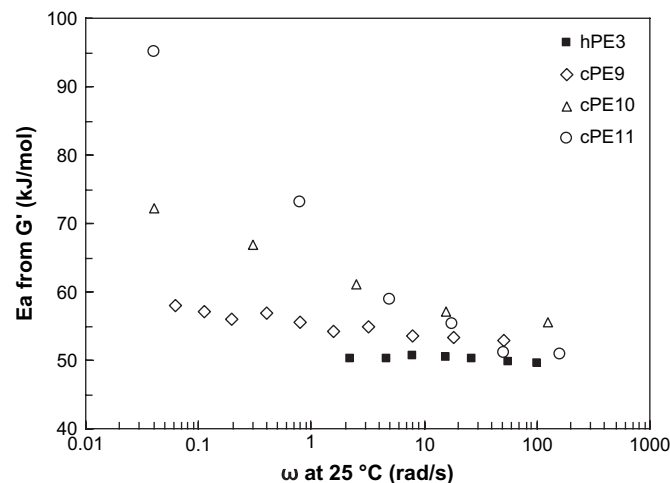


Fig. 12. Activation energy spectra from  $G'(\omega)$  (reference temperature = 25 °C) for the set of polymers synthesized at 35 °C.

the activation energy value of the homopolymer. The higher activation energy values in the low-frequency region should be related to hyperbranched polymers containing significant amounts of intermolecular cross-linking structure, which require longer relaxation times and are more sensitive to temperature [16,29]. In the high-frequency region, the stress relaxation behavior is dominated by the reptation of polymers without intermolecular cross-linking or containing low intermolecular cross-linking densities. Hence the activation energy in this region should converge to approximately the same activation energy for homopolyethylene control samples [16,29].

#### 4. Conclusions

Three sets of hyperbranched polyethylenes containing various cross-linking densities were synthesized by chain walking copolymerization of ethylene with varying but small amounts of 1,4-butanediol diacrylate as cross-linker at three different temperatures, 15, 25, and 35 °C, respectively, using a Pd-diimine catalyst,  $[(ArN=C(Me)-(Me)C=NAr)Pd(CH_3)(N\equiv CMe)]SbF_6$  ( $Ar = 2,6-(iPr)_2C_6H_3$ ). The effective incorporation of the diacrylate is confirmed by  $^1H$  NMR spectroscopy. The molar content of the diacrylate and cross-linking density in the copolymers are positively dependent on both polymerization temperature and the diacrylate feed concentration. Besides the expected intermolecular cross-linking, intramolecular cross-linking was also found to exist in these hyperbranched copolymers. The density of intramolecular cross-linking tends to increase with the increase of polymerization temperature probably due to the increasingly hyperbranched polymer chain conformation resulted.

Triple-detection GPC measurements show that significant enhancement of polymer molecular weight and broadening of molecular weight distribution are resulted due to intermolecular cross-linking. These effects become more pronounced with the increase of diacrylate content. By examining the dependency of intrinsic viscosity on polymer molecular weight, it is found that polymer chain topology becomes more compact, due to intermolecular cross-linking, compared to homopolyethylene control samples. From small-amplitude dynamic oscillatory melt rheological measurements, the hyperbranched copolymers exhibit some characteristic rheological properties typically found in polymers containing intermolecular cross-linking structures, including elevated dynamic moduli, enhanced elasticity, raised viscosity, reduced phase angle, and thermorheological complexity. These rheological properties are more apparent in copolymers containing

higher diacrylate contents (i.e., higher amounts of intermolecular cross-linking structure).

### Acknowledgement

The financial support for this work from the Natural Science and Engineering Research Council of Canada (NSERC) and Imperial Oil Ltd is greatly appreciated. Z.Y. also thanks NSERC and the Canadian Foundation for Innovation (CFI) for funding research equipment and facilities, and Laurentian University for granting a NSERC RCD faculty award.

### Appendix. Supplementary data

GPC elution traces and rheological data of the sets of polymers synthesized at 15 and 25 °C, respectively.

Supplementary data associated with this article can be found in the online version, at [doi:10.1016/j.polymer.2008.06.011](https://doi.org/10.1016/j.polymer.2008.06.011).

### References

- [1] For representative reviews on hyperbranched polymers: (a) Gao C, Yan D. *Prog Polym Sci* 2004;29:183; (b) Voit B. *J Polym Sci Part A Polym Chem* 2000;38:2505.
- [2] For a representative review on dendrimers: Grayson SM, Fréchet JM. *Chem Rev* 2001;101:3819.
- [3] (a) Hong Y, Cooper-White JJ, Mackay ME, Hawker CJ, Malmström E, Rehnberg N. *J Rheol* 1999;43:781; (b) Wang J, Kontopoulou M, Ye Z, Subramanian R, Zhu S. *J Rheol* 2008;52:243.
- [4] Wang J, Ye Z, Zhu S. *Ind Eng Chem Res* 2007;46:1174.
- [5] (a) Varley RJ. *Polym Int* 2004;53:78; (b) Karger-Kocsis J, Fröhlich J, Gryshchuk O, Kautz H, Frey H, Mülhaupt R. *Polymer* 2004;45:1185.
- [6] (a) Gao C, Xu Y, Yan D, Chen W. *Biomacromolecules* 2003;4:704; (b) Kolhe P, Misra E, Kannan RM, Kannan S, Lieh-Lai M. *Int J Pharm* 2003;259:143.
- [7] (a) Fréchet JM, Henmi M, Gitsov I, Aoshima S, Leduc MR, Grubbs RB. *Science* 1995;269:1080; (b) Matyjaszewski K, Gaynor SG, Müller AHE. *Macromolecules* 1997;30:7024; (c) Baskaran D. *Macromol Chem Phys* 2001;202:1569.
- [8] (a) Guan Z, Cotts PM, McCord EF, McLain SJ. *Science* 1999;283:2059; (b) Guan Z. *Chem Eur J* 2002;8:3086.
- [9] (a) Ye Z, Zhu S. *Macromolecules* 2003;36:2194; (b) Ye Z, AlObaidi F, Zhu S. *Macromol Chem Phys* 2004;205:897.
- [10] Plentz-Meneghetti S, Kress J, Peruch F, Lapp A, Duval M, Muller R, et al. *Polymer* 2005;46:8913.
- [11] (a) Chen G, Ma XS, Guan Z. *J Am Chem Soc* 2003;125:6697; (b) Chen G, Huynh D, Felgner PL, Guan Z. *J Am Chem Soc* 2006;128:4298.
- [12] (a) Wang J, Ye Z, Joly H. *Macromolecules* 2007;40:6150; (b) Zhang K, Wang J, Subramanian R, Ye Z, Lu J, Yu Q. *Macromol Rapid Commun* 2007;28:2185; (c) Wang J, Zhang K, Ye Z. *Macromolecules* 2008;41:2290.
- [13] Lashkhi L, Fuks IG. *Chem Technol Fuels Oils* 1988;24:492.
- [14] (a) He Q, Huang H, Bai F, Cao Y. *Macromol Rapid Commun* 2006;27:302; (b) Kulshrestha AS, Gao W, Gross RA. *Macromolecules* 2005;38:3193; (c) Kautz H, Sunder A, Frey H. *Macromol Symp* 2001;163:67; (d) Sun M, Li J, Li B, Fu Y, Bo Z. *Macromolecules* 2005;38:2651.
- [15] (a) Jiang C, Shen Y, Zhu S, Hunkeler D. *J Polym Sci Part A Polym Chem* 2001;39:3780; (b) Gao H, Min K, Matyjaszewski K. *Macromolecules* 2007;40:7763.
- [16] Ye Z, AlObaidi F, Zhu S. *Ind Eng Chem Res* 2004;43:2860.
- [17] (a) Isaure F, Cormack PAG, Graham S, Sherrington DC, Armes SP, Bütün V. *Chem Commun* 2004:1138; (b) Li Y, Armes SP. *Macromolecules* 2005;38:8155.
- [18] Gao H, Matyjaszewski K. *J Am Chem Soc* 2006;128:15111.
- [19] Johnson LK, Killian CM, Brookhart M. *J Am Chem Soc* 1995;117:6414.
- [20] Cotts PM, Guan Z, McCord E, McLain S. *Macromolecules* 2000;33:6945.
- [21] (a) Johnson LK, Mecking S, Brookhart M. *J Am Chem Soc* 1996;118:267; (b) Mecking S, Johnson LK, Wang L, Brookhart M. *J Am Chem Soc* 1998;120:888.
- [22] Liigadas G, Percec V. *J Polym Sci Part A Polym Chem* 2007;45:4684.
- [23] To further confirm the absence of radical induced cross-linking at the polymerization conditions used here, a solution of cPE10 (ca. 0.5 g) in CH<sub>2</sub>Cl<sub>2</sub> (10 mL) was stirred at 35 °C for 24 h (similar to the polymerization condition used) following a reviewer's suggestion. GPC analyses confirmed that the polymer obtained after this stirring procedure had almost identical elution curve and molecular weight data as cPE10, indicating the absence of radical reduced cross-linking at the given polymerization condition.
- [24] (a) Flory PJ. *J Am Chem Soc* 1941;63:3083; (b) Flory PJ. *J Am Chem Soc* 1941;63:3091; (c) Flory PJ. *J Am Chem Soc* 1941;63:3096; (d) Stockmayer WH. *J Chem Phys* 1943;11:45; (e) Stockmayer WH. *J Chem Phys* 1944;12:125.
- [25] Gao H, Li W, Matyjaszewski K. *Macromolecules* 2008;41:2335.
- [26] (a) Taranekar P, Park J-Y, Patton D, Fulghum T, Ramon GJ, Advincula R. *Adv Mater* 2006;18:2461; (b) Lemcoff NG, Spurlin TA, Gewirth AA, Zimmerman SC, Beil JB, Elmer SL, et al. *J Am Chem Soc* 2004;126:11420.
- [27] Ferry JD. *Viscoelastic properties of polymers*. 3rd ed. New York: John Wiley & Sons; 1980.
- [28] (a) Vega JF, Santamaria A, Munoz-Escalona A, Lafuente P. *Macromolecules* 1998;31:3639; (b) Vega JF, Fernandez M, Santamaria A, Munoz-Escalona A, Lafuente P. *Macromol Chem Phys* 1999;200:2257.
- [29] Wood-Adams P, Costeux S. *Macromolecules* 2001;34:6281.